CONFERENCE PRE-PRINT

PROGRESS OF CRAFT NEGATIVE ION SOURCE NEUTRAL BEAM INJECTION TEST FACILITY

J.L. WEI, Y.J. XU, W. LIU, Y.L. XIE, Y.H. XIE, C.C. JIANG, Y.Z. ZHAO, C.D. HU, L.Z. LIANG Institute of Plasma Physics, HFIPS, Chinese Academy of Sciences Hefei, China Email: jlwei@ipp.ac.cn

Abstract

A promising negative-ion-based neutral beam injection (NNBI) system should achieve high energy, high power and long pulse simultaneously for the plasma heating and current drive for the large-scale fusion devices. A NNBI test facility has been constructed in the framework of the Comprehensive Research Facility for Fusion Technology (CRAFT) in China. The installed capability of the whole CRAFT NNBI test facility is the beam energy of 400 keV, the ion beam current of 28 A, and the continuous beam pulse of 1 hour. A dual-driver RF negative ion source (beam size: 0.75×0.3 m2, design acceleration voltage: 200 kV) has been developed and tested for the first operation of the test facility. Several significant improvements were applied to the test facility or the negative ion source during the system maintenance, such as the insulation of the transmission line for electric power and cooling water, the total pumping area of the cryopumps, the high-voltage holding of the negative ion source, the cesium injection system. In the second experimental campaign of CRAFT NNBI test facility, the repeatable 100 seconds and megawatt negative hydrogen ion beams have been achieved at the filling pressure of 0.4 Pa and the typical values were 135 keV, 10.6 A ($\approx180 \text{ A/m2}$) and 110 s. For ten second beam pulses the higher energy and higher power was established (173 keV and 12 A). The results demonstrated the negative ion source can reliably operate in a medium beam parameter for long pulse. Some problems about the high-voltage holding, particle and heat flux were revealed in the high-power and long-pulse beam acceleration.

1. INTRODUCTION

Neutral beam injection (NBI) with energic deuterium (or its isotopes) is a powerful and straightforward method for the plasma heating and current drive in the magnetic confinement fusion (MCF) devices. NBI is the strong guarantee for producing high-parameter plasmas in several milestones of the MCF development history [1-7]. The long-pulse operation will be a basic requirement for the NBI application to the future fusion reactors in different functions [8-13]. Even for the ion-heating and plasma ignition during the ramp-up phase, the neutral beam is needed to continuously inject for hundreds of seconds.

The long-pulse and high-power operation has been verified in several positive-ion-based NBI (PNBI) systems. Those PNBI systems are generally applied to the fusion devices based on superconducting magnets [14-17]. But for larger fusion devices, the required injecting beam energy is also higher to obtain the effective core plasma heating and current drive. For example, the ITER heating neutral deuterium beam is required to inject at the beam energy up to 1 MeV; the injection power and the pulse duration are 16.5 MW and 1 hour respectively [18]. At such a high beam energy, the negative-ion-based NBI (NNBI) system is more practical due to its acceptable neutralization yield of ~55% [19].

The PNBI and NNBI systems are simultaneously equipped on the JT-60U tokamak and the LHD heliotron. Their NNBI systems, especially the negative ion sources, have proved to be much more complex and challenging. Although those negative ion sources were designed to be operated for around 10 s, they were still put into long-pulse operation (tens of seconds) and some prominent problems arose: the instability of the amount or uniformity of the extracted negative ions and electrons, the frequent breakdowns before the ending of the beam acceleration, and the local deformations or erosions on the accelerator due to the particle and heat flux [20,21].

There are several test facilities to develop the long-pulse operation of the negative ion sources. The ELISE test facility at IPP-Garching is devoted to demonstrating that the key design values of the ITER negative ion source can be fulfilled. Its half-ITER-size ion source (cross-section: 1×1 m2, 640 apertures, extraction area: 0.1 m2) achieved the long-pulse (600 s) and high-current (~30 A) extraction of negative hydrogen ion beams [22,23]. One significant contribution of the ELISE is to suppress the increase of the number and the inhomogeneity of the co-extracted electrons during the long-pulse operation. But the acceleration voltage on the ELISE is limited to only around 50 kV.

The MeV test facility (MTF) at QST-Naka is devoted to the physics and engineering issues about the high-energy acceleration of negative ions. By using the ITER-like and the JT-60SA-like multi-aperture and multi-grid (MAMuG) accelerators, the negative hydrogen ions were accelerated to 0.97 MeV for pulse duration of 60 s with the current density of 190 A/m2 and to 0.5 MeV for lasting 118 s with 154 A/m2, respectively [24,25]. One effort on the MTF is to stabilize the negative ion production during the long-pulse operation via the careful control of the Cs wall condition. But the source size is small and the beam current is limited to only 0.5 A on the MTF.

The ITER Neutral Beam Test Facility (NBTF) is hosted at Consorzio RFX and includes two test-beds: SPIDER, the full-size radio frequency negative-ions source, and MITICA, the full-scale prototype of the ITER heating neutral beam injector. The SPIDER and its full-ITER-size negative ion source (cross-section: 2 × 1 m2, 1280 apertures, up to 100 keV) have finished the first long-term campaign of around 3.5 years. Due to the insufficient gas pumping, the source was operated with a reduced extraction area (28 apertures opening), so neither the long-pulse nor high-power operation of the negative ion beam was demonstrated. Meanwhile the MITICA is still under construction: the 1 MV acceleration grid power supply and the related high-voltage transmission lines, bushing and insulating transformer have been implemented the first integrated tests; the vacuum vessel of the injector has been installed but the in-vessel components, such as beam source, beamline components and cryopump are still on procurement [26,27].

A NNBI test facility has been constructed in 2023 at ASIPP under the CRAFT project (Comprehensive Research Facility for Fusion Technology) [28]. CRAFT is an integration of different test facilities or systems for testing and validating the method, standard, and technology for a successfully construction and operation of the he next-generation Chinese MCF device, CFETR (China Fusion Engineering Test Reactor). The differentiation and synergy of the CRAFT NNBI test facility to other test facilities worldwide for negative ion source or NNBI are considered during the project initiation stage. Its design baseline is to demonstrate a 200-400 keV, 2-4 MW, 100-3600 s neutral hydrogen beam. The CRAFT NNBI test facility contains two test stands: HONOR (Hefei Openfacility for Negative-ion Source Research) focuses on the negative ion source research for fusion; CANBE (CFETR Advance Neutral Beam Equipment) is a full-function prototype for the CFETR neutral beam injector. Hence, only the CANBE can produce the neutral beam, but the HONOR is equipped with more plasma and beam diagnostic systems. The HONOR and CANBE share the same acceleration grid power supply, cooling water system and cryogenic system. Specially, the acceleration voltage of HONOR is limited to 200 kV to simplify the high-voltage power transmission and insulation.

2. EXPERIMENTAL SETUP

The 2nd experimental campaign of the CRAFT NNBI test facility is mainly carried out on the CANBE test stand, as shown in figure 1(a). The CANBE beamline has a similar structure with the ITER heating neutral beam injector. The vacuum vessel is rectangular with 12 m in length, 4 m in width and 4 m in height. It's divided into three individual parts along the beam direction, inside which are installed with the gas neutralizer, the electrical-based residual ion dump and the beam dump in turn. In addition, two cryo-sorption pumps are installed on the lateral walls.

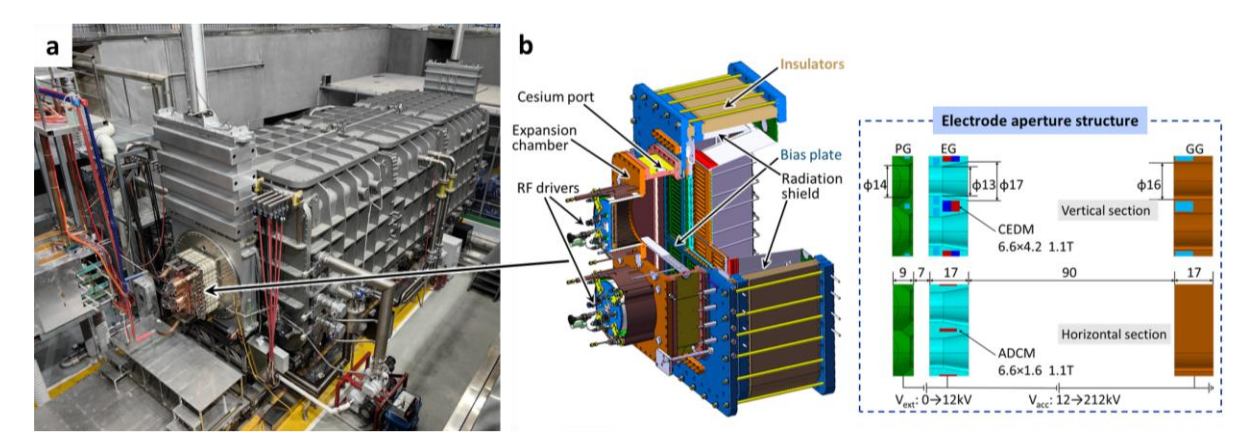


FIG. 1. (a) Photograph of the CANBE test stand and the dual-driver negative ion source. The whole source works in the air and connects to the beamline with a gate valve. (b) Cut-away diagram of the dual-driver negative ion source and structure of the grid apertures.

A cut-away diagram of the CRAFT dual-driver negative ion source is shown in Figure 1(b). New concept or unique design of negative ion source has not yet reached the practical application at ASIPP. The designs of CRAFT dual-driver negative ion source are inherited from the CRAFT single-driver negative ion source [29-31], which was based on the designs of the ITER negative ion source and the research results of IPP, QST-Naka, NIFS, Consorzio RFX, IRFM and so on. A large-area negative ion generator of IPP-type is adopted. The low-pressure plasmas are generated from two cylindrical RF drivers, and then diffuse and mix in the expansion chamber. Two identical RF power supplies of 200 kW are available and the RF frequency is 1 MHz. The cross-section of the expansion chamber is 90×50 cm2. The lateral walls of the expansion chamber are surrounded by the confining magnets with a checkerboard arrangement to enhance the plasma density [32]. Most of the extracted negative ions are generated via the collisions of hydrogen atoms or ions on the plasma grid (PG), which is covered by the cesium with a low work function. In the dual-driver negative ion source, the cesium is evaporated from the bending nozzle on the top or bottom wall which points to the backplate of the expanding chamber [33]. Nevertheless, the continuous injecting cesium can be re-distributed by the plasma and the back-streaming particles and deposited onto the top surface of PG [34].

The magnetic filter field is a common design in the negative ion source. It's used to reduce the electron temperature and electron density in front of the PG, to suppress the collisional loss of the negative ions and the co-extraction of the electrons. In the dual-driver negative ion source, the transverse filter field is produced via the electric current flow through the PG in the vertical direction. No return wires or current bars for adjusting field shape like ELISE or SPIDER is used [35]. A bias plate (BP) with two segments is placed and insulated between the expansion chamber and the PG. According to the experience on the single-driver negative ion source, a positively bias voltage was applied on the PG against the expansion chamber (meanwhile, the BP was floated). The PG bias was necessary during the initial cesium conditioning to reduce the co-extracted electrons; in the sufficient cesium conditioning stage, it was still useful to optimize the local potential for negative ions generation and extraction [36].

A three-grid and multi-aperture accelerator is applied to the dual-driver negative ion source. Each grid electrode is divided into two segments and each segment includes two aperture groups (corresponding to the rectangular openings of BP). The negative ions near the PG are extracted through a total of 384 apertures (\$\phi14\$ mm) by the electric field between the PG and the extraction grid (EG). Applying a relatively low extraction voltage (up to 12 kV) is because the EG has to dump the co-extracted electrons and the power deposition must be limited [37]. The asymmetric magnetic fields are formed by the Halbach-like magnets array inside the EG to deflect the co-extracted electrons onto the EG [38]. Such fields can reduce the deflection of negative ion beamlets that induced by the unbalanced magnetic moments between the upstream and the downstream side of EG. One of the probable causes was that the suppression on the co-extracted electrons by the EG magnets was weakened when enlarging the extraction gap [39]. The negative ions are further accelerated between the EG and the ground grid (GG). Particularly, the GG adopts the multi-slot apertures, to reduce the interception of energic particles on the GG [40]. A field shaping plate (FSP) is attached on the downstream side of EG to reduce the whole beam divergence induced by the multi-beamlet repulsion [41].

3. EXPERIMENTAL RESULTS

The improvements or changes for the second campaign focused on the high-voltage holding, vacuum pumping and water cooling of the whole test facility. The only but critical modification of the negative ion source was the radiation shield inside the accelerator (shown in Figure 1(b)). The stainless steel made radiation shields of different dimensions were tested in the beam acceleration with a reduced extraction area (240 apertures) and without the cesium seeding. The experimental results are summarised in Figure 2. It indicates that the radiation shield has a great influence on the high voltage holding. In the cases of without or short radiation shield, the low breakdown voltage was attributed to the direct deposition of the radiation or stray particles onto the inner surfaces of the insulator from the grids. In the case of high radiation shield, the acceleration voltage was limited to 152 kV. The sparks that recorded by the video camera and the discharge traces on the inner surfaces revealed that the frequent breakdowns occurred between the radiation shield and the fibre enhanced epoxy insulator.

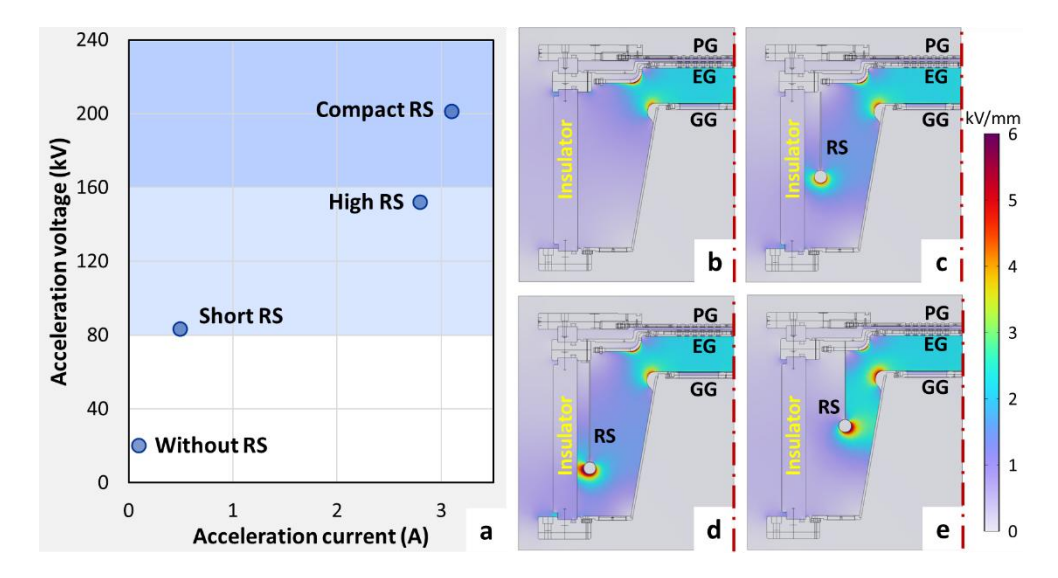
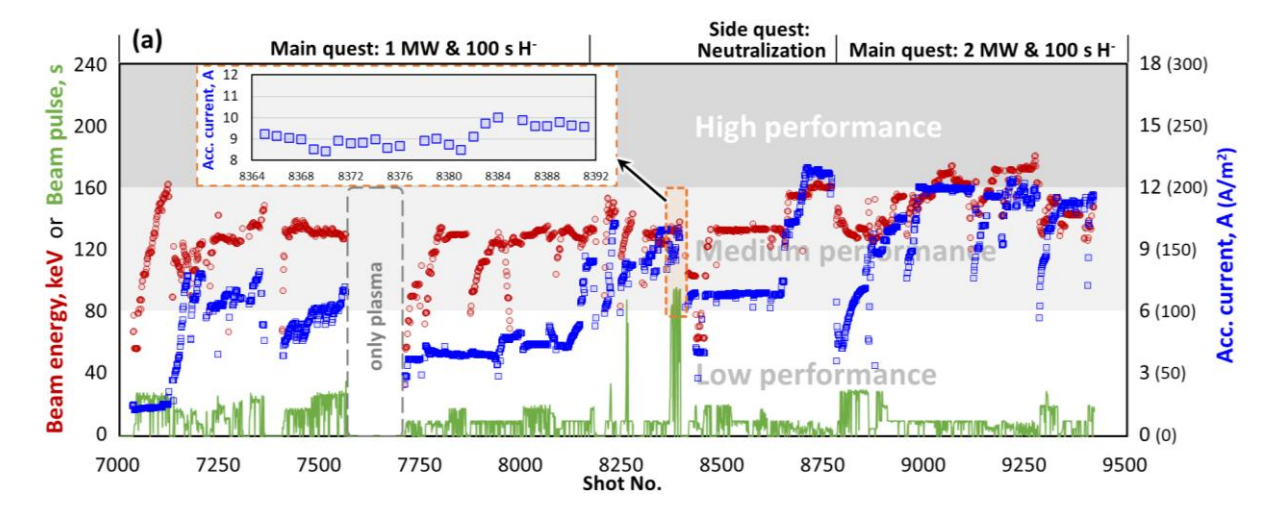


FIG. 2. (a) Achieved acceleration voltage of the dual-driver negative ion source with different radiation shields (RS). Those testing were done without cesium seeding to eliminate its influence on high voltage holding. (b-e) Electric field distribution of the accelerator with different RS (b: without RS, c: short RS, d: high RS, e: compact RS). The acceleration voltage was set to 200 kV in the electric field simulations.

In the 1st experimental campaign of the CRAFT NNBI facility, the best values of the negative ion beam were 135.9 keV, 8.9 A (~150 A/m2), 8 s that also achieved by the dual-driver negative ion source. One of the main quests of the 2nd experimental campaign is to extend a similar power of negative ion beam (>1 MW) to at least 100 s. This main quest lasted for 3 weeks and the variations of the key beam parameters are shown in Figure 3(a). In those experiments, the RF coils of the two drivers were connected in series; the PG was cooled by the room-temperature, because the high-temperature water supply system still could not work (damaged by high voltage breakdown in the 1st campaign). At the beginning, the beam energy was increased gradually to ~165 keV for the high voltage conditioning of the source and the whole system. And then, the ion beam power was raised to >1 MW for 20~30 s. However, a water leaking was found on one cooling pipe of the GG, which took 3 days to be repaired. Based on the experience of single-driver negative ion source, the polluted cesium in the air was not cleaned up from the surfaces of the expansion chamber and the PG. They could be re-activated by the plasma and the beam acceleration could be easily restarted at the ion current density of ~50 A/m2.



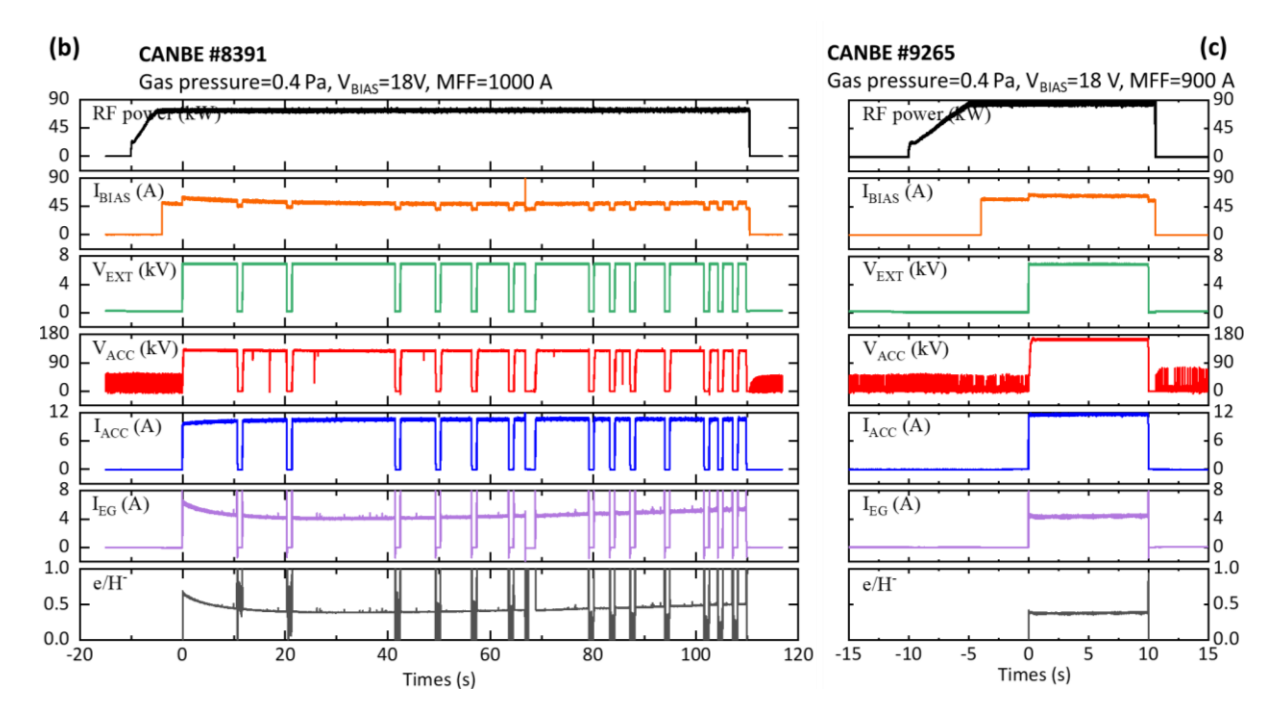


FIG. 3. (a) Variation of key beam parameters (i.e., beam energy, acceleration current, pulse duration) during the main quest for high-power and long-pulse acceleration of negative hydrogen beam in the second experimental campaign of CRAFT NNBI facility. Evolution of acceleration current in different long-pulse shots are zoomed in. (b) Typical waveforms of long-pulse shot with the ion beam power above 1 MW. (c) Typical waveforms of short-pulse shot with the ion beam power above 2 MW.

The ion beam power was lifted again but more slowly. A negative ion beam with 1.1 MW for lasting 105 s was obtained on the fifth day since the experiment restart. On the sixth day, the long-pulse shots with a higher ion beam power of 1.4 MW could be achieved repeatedly. The typical waveforms of the long-pulse shot and the main operation parameters are shown in Figure 3(b). Note that, the filling gas pressure of 0.4 Pa was selected to maintain the more stable RF plasma discharges with cesium seeding, although the gas pressure should be as low as possible to reduce the stripping loss of negative ions. The achieved beam energy was 134.9 keV, the acceleration current given by the acceleration voltage power supply was 10.6 A (~179 A/m2), and the pulse duration was 110 s. The most eye-catching was the 14 times of breakdown, but only once was due to the acceleration (at around 67 s with longer restart interval time). Such many extraction breakdowns were abnormal. A manufacturing and assembly error was found in the disassembly inspection after the campaign that the distance between the busbar of the PG current and the EG supporting frame was only ~2 mm. Here, the current flow onto the EG was regarded as the co-extracted electron current. In the first 20 s, the acceleration current increased gradually but the EG current decreased more sharply, which made the electron-to-ion ratio dropped off from 0.7 to 0.3. It could be result of the re-distribution of the cesium by the plasma and the backstreaming ions. Due to the water-cooled PG and the medium ion current density, a possible degradation of the acceleration current didn't happen. But the co-extracted electrons did continue to increase after 40 s and the extraction breakdowns became frequent near the end of the pulse.

And then, the campaign moved to a side quest to study the gas neutralization of the negative ion beams. Its details have been described and discussed in the Ref. [42]. Briefly, the achieved neutralization efficiency and its relation to the gas inlet rate was well consistent with the beam-gas simulations; however, the frequent high-voltage breakdowns on the residual ion dumps leaded to the insufficient neutralization of the negative ions at the energy of >150 keV.

The campaign was got back to the subject of the high-power and long-pulse negative ion beam acceleration. An unexpected degradation of the extracted negative ions occurred in the first day of that main quest; meanwhile, the interlock protection due to the RF reflection became frequent. Then, the cesium injection was closed to reduce the RF plasma instability. On the other hand, the long-pulse ion beam accelerations (~30 s) were repeated to recover the cesium condition near the PG [43]. The beam current density was gradually increased back to 150 A/m2 and the RF breakoff also disappeared. The cesium injection was reopened in the following days to realize a high-

current beam. And the reference shot for the high-power ion beam acceleration of >2.0 MW was established, as shown in Figure 3(c). The beam energy was 172.9 keV, the acceleration current was 12.1 A (~203 A/m2), and the pulse duration was 10 s. The electron-to-ion ratio could be suppressed under 0.3. The achieved acceleration voltage of 166 kV has reached one-third of the requirement of a 500-keV and three-stage accelerator, which is under design for the NNBI system of a burning plasma tokamak in China.

An interim target of the 1.7 MW and 100 s negative ion beam acceleration must be attained at first. The 20 s shots at such beam power (extraction voltage: 6.8 kV, acceleration voltage: 145 kV, beam current: 11.7 A) were very stable and replicate. However, a water-leaking failure inside the beamline stopped the experimental campaign. The leakage points located at the leading-edge element (LEE) of the middle panel of the neutralizer, as shown in Figure 4(a). The middle panel was used to form two narrow gas cells and the LEE has been carefully designed to bear the heat load from the beam halo and stripping electrons [44,45]. This failure resulted in a pause of one month because the adsorbent of the cryopumps absorbed too much water. Although the experiments of beam acceleration were restarted, the turbine of the cryogenic system was malfunctioned soon and the whole campaign was stopped.

The postoperative analysis found that the whole negative ion beam was probably overfocused due to the electric field distortion induced by the grid supporting frames. Figure 4(b) shows the distribution of electric potential inside the accelerator. The supporting frame of GG and the radiation shield formed a radial electric field, which had already affected the parallelism of the electric field between EG and GG. The ion trajectories of the 1.7 MW beam were simulated under the full-size accelerator. The horizontal deflection angle of each beamlet from the top half is shown in Figure 4(c), and all the beamlets indicate an incurvate deflection. That is the beamlets of the left group shift to the right-hand side and the right group is opposite. The average deflection angle of the middle two column of beamlets is 7.2 mard and -6.9 mrad. The distance from the GG to the neutralizer entrance is ~2.0 m, so the average deviations of those middle beamlets are ~14 mm and all point to the LEE.

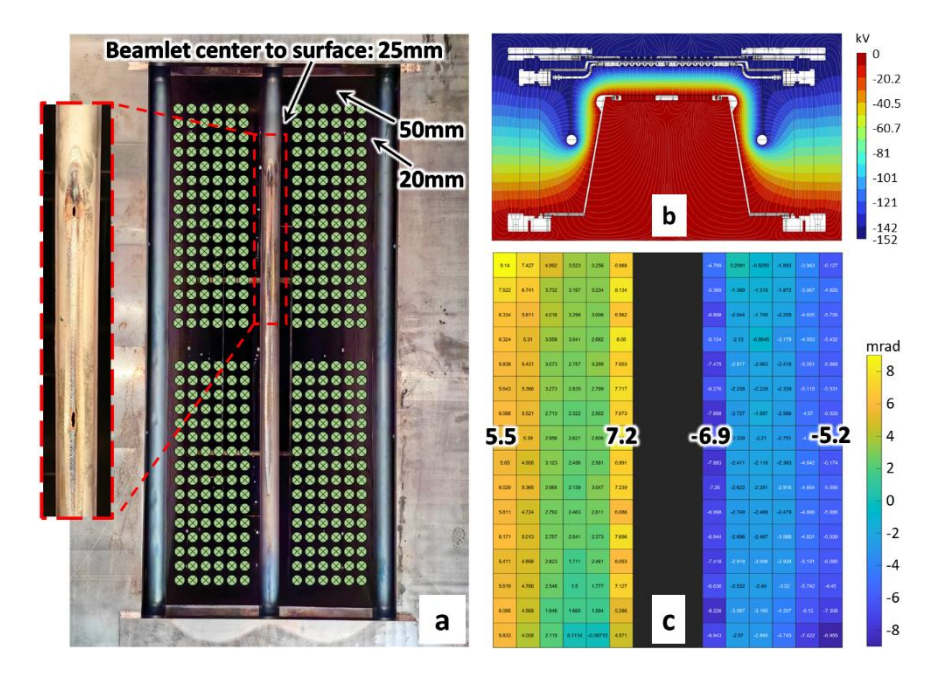


FIG. 4. (a) Pictures of the entrance of the neutralizer after high-power and long-pulse beam operation; the melting and water-leaking points on the leading-edge element of the middle panel are zoomed in; the layout of all beamlets and the distances of the lateral beamlet center to the panel surface are also indicated. (b) Distribution of electric potential and horizontal deflection angle of each beamlet in the full-size accelerator for the negative ion beam parameters of 152.8 keV and 11.7 A. (c) The average deflection angle of the 1st, 6th, 7th and 12th line of beamlets is indicated respectively.

4. CONCLUSIONS AND NEXT PLANS

The CRAFT NNBI facility aims to develop the key technology of the high-energy, high-current and long-pulse negative ion beam acceleration or neutral beam injection (only on CANBE test stand). Its design operating parameters (up to 400 kV, 25 A, 3600 s) are complemented with the other long-pulse test facilities for the negative ion source (e.g., ELISE, MTF, SPIDER). A negative hydrogen ion beam of 110 s and 1.4 MW has been achieved via a dual-driver RF negative ion source with single-stage accelerator. The beam parameters were in the medium

level that the beam energy was 134.9 keV and the ion current density was ~179 A/m2. And such long-pulse and high-power beam accelerations can be attained repeatedly and continuously. The higher beam power of >2 MW has been also established in short pulse (beam energy: 172.9 keV, ion current density: 203 A/m2), but its long-pulse testing was forced to stop because of the water-leaking failure on the neutralizer. The post-operative disassembly indicated that: (1) Grid supporting frames (including the radiation shields) have an obvious influence on the overall beam optics, which should be carefully estimated especially for the multi-channel neutralizer. (2) Particle and heat flux on the grid supporting frames became a decisive factor in the high-power and long-pulse beam acceleration.

The current version of CRAFT dual-driver negative ion source was based on an ITER-like design from the public papers or reports, combining with the worldwide research experience on the negative ion source for NBI. Hence, the present results can also partly verify the design or operation method of the ITER negative ion source. Next step, several developing techniques will be applied to the dual-driver negative ion source to demonstrate the actual operation capability, for example, the RF plasma discharge with higher frequency above 1 MHz, the active cooling RF driver without Faraday shield, the ferromagnetic plate attached on the back plate of expansion chamber, the filter field shaping with multiply electric bars [48-50]. To deal with the particle and heat flux problems, the EG will be coated by the molybdenum layer and the supporting frames of GG will be added the water-cooling structure. The chase for the higher beam parameters (e.g., >200 keV and >250 A/m2) in long pulse depends on the key physics issues that stability of negative ions generation, uniformity of plasma or beam, suppression of co-extracted or stripping electrons, minimization of beam divergence and misalignment. Those physics research will be carried out on the HONOR in terms of priority because it has been equipped with various plasma and beam diagnostics [51].

ACKNOWLEDGEMENTS

This work has been carried out within the framework of the CRAFT NNBI Physics Activity and supported by the Comprehensive Research Facility for Fusion Technology Program of China (No.2018-000052-73-01-001228).

REFERENCES

- [1] Eubank H et al 1979 Phys. Rev. Lett. 43 270-274. https://doi.org/10.1103/PhysRevLett.43.270
- [2] Wagner F et al 1982 Phys. Rev. Lett. 49 1408-1412. https://doi.org/10.1103/PhysRevLett.49.1408
- [3] Hawryluk R.J. 1998 Rev. Mod. Phys. 70, 537-587. https://doi.org/10.1103/RevModPhys.70.537
- [4] Rimini F G et al 2025 Plasma Phys. Control. Fusion 67 033001. https://doi.org/10.1088/1361-6587/adaee5
- [5] Fujita T et al 1999 Nucl. Fusion 39 1627-1636. https://doi.org/10.1088/0029-5515/39/11y/302
- [6] Han H et al 2022 Nature 609 269-275. https://doi.org/10.1038/s41586-022-05008-1
- [7] Ding S et al 2024 Nature 629 555-560. https://doi.org/10.1038/s41586-024-07313-3
- [8] Polevoi A R et al 2020 Nucl. Fusion 60 096024. https://doi.org/10.1088/1741-4326/aba335
- [9] Chen J L et al 2021 Nucl. Fusion 61 046002. https://doi.org/10.1088/1741-4326/abd7b8
- [10] Vincenzi P et al 2021 Plasma Phys. Control. Fusion 63 065014. https://doi.org/10.1088/1361-6587/abf402
- [11] Sugiyama S et al 2024 Nucl. Fusion 64 076014. https://doi.org/10.1088/1741-4326/ad49b6
- [12] Mikkelsen D R et al 2018 Nucl. Fusion 58 036014. https://doi.org/10.1088/1741-4326/aaa4d2
- [13] Hopf C et al 2021 Nucl. Fusion 61 106032. https://doi.org/10.1088/1741-4326/ac227a
- [14] Ikeda Y et al 2007 Fusion Eng. Des. 82 791-797. 10.1016/j.fusengdes.2007.05.077
- [15] Kojima A et al 2016 Fusion Eng. Des. 102 81-87. 10.1016/j.fusengdes.2015.11.033
- [16] Chang D H et al 2012 Curr. Appl. Phys. 12 1217-1222. https://doi.org/10.1016/j.cap.2012.02.063
- [17] Xie Y H et al 2023 Fusion Eng. Des. 193 113744. https://doi.org/10.1016/j.fusengdes.2023.113744
- [18] Hemsworth R S et al 2017 New J. Phys. 19 025005. https://doi.org/10.1088/1367-2630/19/2/025005
- [19] Hemsworth R S and Inoue A 2005 IEEE Trans. Plasma Sci. 33 1799-1813. https://doi.org/10.1109/TPS.2005.860090
- [20] Hanada M et al 2008 22nd IAEA Fusion Energ. Conf. FT/P2-27
- [21] Takeiri Y et al 2006 Nucl. Fusion 46 S199-S210. https://doi.org/10.1088/0029-5515/46/6/S01
- [22] Fantz U et al 2024 Nucl. Fusion 64 086063. https://doi.org/10.1088/1741-4326/ad5dcd
- [23] Wünderlich D et al 2025 Nucl. Fusion 65 014001. https://doi.org/10.1088/1741-4326/ad8e74
- [24] Kashiwagi M et al 2022 Nucl. Fusion 62 026025. https://doi.org/10.1088/1741-4326/ac388a
- [25] Kashiwagi M et al 2022 Rev. Sci. Instrum. 93 053301. https://doi.org/10.1063/5.0080804

IAEA-CN-316/2982

- [26] Sartori E et al 2022 Nucl. Fusion 62 086022. https://doi.org/10.1088/1741-4326/ac715e
- [27] Marcuzzi D et al 2023 Fusion Eng. Des. 191 113590. https://doi.org/10.1016/j.fusengdes.2023.113590
- [28] Wei J L et al 2025 Plasma Sci. Technol. 27 044001. https://doi.org/10.1088/2058-6272/ad8da7
- [29] Gu Y M et al 2021 Fusion Eng. Des. 171 112600. https://doi.org/10.1016/j.fusengdes.2021.112600
- [30] Xie Y H et al 2023 J. Instrum. 18 C07017. https://doi.org/10.1088/1748-0221/18/07/C07017
- [31] Yang Y W et al 2024 Plasma Phys. Control. Fusion 66 055019. https://doi.org/10.1088/1361-6587/ad3c1e
- [32] Chen Y Q et al 2024 Fusion Eng. Des. 199 114149. https://doi.org/10.1016/j.fusengdes.2024.114149
- [33] Wu Y et al 2024 IEEE Trans. Plasma Sci. 52 3693-3697. https://doi.org/10.1109/Tps.2024.3353757
- [34] Yang Y L et al 2024 Nucl. Eng. Technol. 56 1145-1152. https://doi.org/10.1016/j.net.2023.11.019
- [35] Heinemann B et al 2019 Fusion Eng. Des. 146 455-459. https://doi.org/10.1016/j.fusengdes.2018.12.090
- [36] Peng X F et al 2023 Phys. Plasmas 30 103507. https://doi.org/10.1063/5.0156271
- [37] Wang J H et al 2025 Nucl. Eng. Technol. 57 103182. https://doi.org/10.1016/j.net.2024.08.051
- [38] Chitarin G et al 2014 Rev. Sci. Instrum. 85 02B317. https://doi.org/10.1063/1.4826581
- [39] Tsumori K et al 2022 Nucl. Fusion 62 056016. https://doi.org/10.1088/1741-4326/ac2d59
- [40] Tsumori K et al 2004 Rev. Sci. Instrum. 75 1847-1850. https://doi.org/10.1063/1.1702107
- [41] Ikeda Y et al 2006 Nucl. Fusion 46 S211-S219. https://doi.org/10.1088/0029-5515/46/6/S02
- [42] Li B et al 2025 Nucl. Sci. Tech. Accepted
- [43] Kojima A et al 2017 Fusion Eng. Des. 123 236-240. https://doi.org/10.1016/j.fusengdes.2017.01.060
- [44] Yi W et al 2023 Fusion Eng. Des. 194 113749. https://doi.org/10.1016/j.fusengdes.2023.113749
- [45] Wei J L et al 2021 Fusion Eng. Des. 169 112482. https://doi.org/10.1016/j.fusengdes.2021.112482
- [46] Wei J L et al 2023 Phys. Plasmas 30 033102. https://doi.org/10.1063/5.0139827
- [47] Yang Y W et al 2023 Nucl. Eng. Technol. 55 939-946. https://doi.org/10.1016/j.net.2022.12.002
- [48] Xing S Y et al 2024 Nucl. Fusion 64 056015. https://doi.org/10.1088/1741-4326/ad34e3
- [49] Liu B et al 2024 Rev. Sci. Instrum. 95 103515. https://doi.org/10.1063/5.0219356.
- [50] Xie J W et al 2025 Phys. Plasmas 32 013110. https://doi.org/10.1063/5.0245538.
- [51] Xu Y J et al 2025 Fusion Eng. Des. 211 114808. https://doi.org/10.1016/j.fusengdes.2025.114808